Research Article

Chemical Review and Letters
journal homepage: www.chemrevlett.com
ISSN (online): 2645-4947 (print) 2676-7279

A computational comparison into the cation–π interaction and its effect on the intramolecular hydrogen bond in the different complexes of 5-Aminosalicylic acid with its thio analogous

Manal Morad Karim[1], Nada Othman Kattab[2], Hala Bahir[3], Ayat Hussein Adhab[4], Azadeh Khanmohammadi[5, *]

[1] *College of Dentistry, National University of Science and Technology, Dhi Qar, Iraq*
[2] *Department of Radiology & Sonar Techniques, Al-Noor University College, Nineveh, Iraq*
[3] *Medical technical college, Al-Farahidi University, Iraq*
[4] *Department of Pharmacy, Al-Zahrawi University College, Karbala, Iraq*
[5] *Department of Chemistry, Payame Noor University (PNU), P.O.Box 19395-4697, Tehran, Iran*

ARTICLE INFO

Article history:
Received 11 Septeber 2023
Received in revised form 31 December 2023
Accepted 31 December 2023
Available online 31 December 2023

Keywords:
Cation-π
Intramolecular hydrogen bond
DFT
AIM
NBO

ABSTRACT

The effects of non-covalent interactions on the strength and nature of the 5-Aminosalicylic acid complexes and its thio analogous are investigated at the ωB97XD/6-311++G(d,p) level of theory. The atoms in molecules and the natural bond orbital analyses are applied for a better understanding of these interactions. The results show that the cation-π interactions in the monovalent complexes have a stronger influence on the HB strength with respect to those in the divalent complexes. The replacement of oxygen by sulfur atoms increases the hydrogen bond strength in the complexes. Based on the molecular orbital data, the Li^+ complexes with the larger energy gap are more stable and harder, while the Mg^{2+} complexes with the lower energy gap are more reactive and thus softer.

1. Introduction

5-Aminosalicylic acid (5-ASA), also known as mesalazine or mesalamine, is structurally related to salicylates and non-steroidal anti-inflammatory drugs like acetylsalicylic acid [1]. Aminosalicylates are a group of drugs that are commonly utilized to therapy intestinal diseases [2]. For instance, the ASA is used to treat ulcerative colitis (a condition that causes swelling and sores in the lining of the colon [large intestine] and rectum) and Crohn's disease (effective only in colonic diseases) [3, 4]. It acts by stopping the body from producing a certain substance that may cause inflammation. In patients with inflammatory bowel disease, there is increased migration of leukocytes, abnormal production of cytokines, amplified production of arachidonic acid metabolites, especially leukotriene B4, and augmented free radicals' formation in inflamed intestinal tissue. The ASA has in-vitro and in-vivo pharmacological effects that inhibit leukocyte chemotaxis, decrease cytokine and leukotriene production, and scavenge free radicals [5, 6].

Non-covalent interactions (NCIs) play a major role in many foremost areas of modern chemistry, from materials design to molecular biology [7-10]. Some of the main types of NCIs studied in the complexes are ionic bonds, hydrophobic interactions, hydrogen bonds, and van der Waals forces (dispersion attractions, dipole-dipole, and dipole-induced dipole interactions). One of the most significant intermolecular/intramolecular weak interactions that have been extensively considered in chemistry as well as in biology is hydrogen bonding (HB) [11-14]. From the sum of four different forces of electrostatic (E_{el}), polarization (E_{pol}), charge transfer (E_{ct}), and dispersion (E_{disp}), the total energy of an HB system can be evaluated. The electrostatic interactions and polarizations are the main contributors participating in the strong HBs. By increasing the covalent properties,

∗ Corresponding author.; e-mail: az_khanmohammadi@yahoo.com
https://doi.org/ 10.22034/crl.2023.416005.1247

the softness of HB is enhanced; and in this case, the vital contributors are reflected in the charge transfer and van der Waals force (dispersion) [15-18]. The nature of X and A atoms (X–H···A) plays a crucial role in the influence of the mentioned forces on the strength of HB.

The cation–π interactions, as another ensemble of NCIs, refer to the binding of cations to π molecules [19-24]. They play a key role in protein folding [25], ion selectivity [26], molecular recognition [27], self-organized electronic materials [28] and organic nanodevices [29]. Several factors are assumed to affect the cation–π interactions. The electrostatic and polarization contributions are dominant in the cation–π interactions, while the dispersion component in these interactions is minimal [30, 31]. The induction term also recovers the interaction of the permanent multipole moments of one monomer with the induced multipole moments on the other monomer.

The exploration of NCIs is an interesting subject from theoretical and experimental viewpoints [32-43]. The influence of cation-π interaction on intramolecular hydrogen bonding (IMHB) has been studied in many systems. For example, Mohammadi et al. [44] investigated NCIs in the various complexes of methyl salicylate and Li^+, Na^+, K^+, Be^{2+}, Mg^{2+}, and Ca^{2+} cations. They observed the reducing effect of the cation-π interaction on the IMHB in the considered complexes. They [45] also conducted a theoretical investigation on the NCIs of mesalazine complex with the presence of Mn^+, Fe^{2+}, Co^+, Ni^{2+}, Cu^+, and Zn^{2+} different cations. The results indicated that, in most cases, the IMHB is weakened by the cation–π interaction in the selected complexes. Also, the influence of cation-π interactions on the strength and nature of IMHB in orthohydroxy benzaldehyde complexes was examined by Khanmohammadi et al. [46].

The role of metal ions in regulating the structure and function of small and large molecules is undeniable [47]. Alkali and alkaline earth metal ions are omnipresent in surviving systems and numerous cases of their central role exist in biological processes [48, 49]. In the present study, the NCIs are considered in the modeling by Li^+, Na^+, K^+, Mg^{2+}, Ca^{2+} ions with ASA and its thio analogous (TASA) as π–systems. The geometrical parameters, binding energies, topological properties, and charge transfer quantities are examined to gain further insight into the effects of NCIs on the selected complexes. Here, the DFT calculations and the AIM and NBO analyses are utilized for a better understanding of these interactions. The effect of the cation–π interaction on the IMHB has also been investigated in the studied complexes. Finally, the DFT-based reactivity and stability descriptors are utilized to estimate the electronic properties of the titled complexes.

2. Quantum chemical calculations

The geometry optimizations and the vibrational frequency calculations are performed with the ωB97XD method [50] and 6-311++G(d,p) basis set [51]. The Gaussian 09 program [52] is used to carry out all these calculations. The binding energies (ΔE) of A (ASA or TASA) and B (metal ions) monomers are computed as the energy difference between the complexes and the corresponding donor–acceptor moieties. For the selected systems, the binding energy is defined as the following equation:

$$\Delta E = E_{AB} - (E_A + E_B) \quad (1)$$

where E_{AB} is the energy of complexes, E_A is the energy of ASA (or TASA) monomer, and E_B is the energy of metal ions. The basis set superposition error (BSSE) [53] is taken into account by the counterpoise (CP) scheme to correct the obtained binding energies. The atoms in molecules (AIM) analysis [54] is applied to evaluate the bond critical points (BCPs) in terms of electron density and its Laplacian. The AIM calculations are performed with the AIM2000 program [55] on the wave functions obtained at the ωB97XD/6-311++G(d,p) level. The population analysis is also done by the natural bond orbital (NBO) method [56] at the same level of theory. To evaluate the electronic properties of the considered complexes, the highest occupied molecular orbital (HOMO) and the lowest unoccupied molecular orbital (LUMO) energies are estimated by the ωB97XD method and the 6-311++G(d,p) basis set. These energies are applied for determining the global chemical reactivity descriptors of complexes such as softness (S), hardness (η) [57], electronic chemical potential (μ) [58], electronegativity (χ) [59] as well as global electrophilicity power (ω) [60]. Using Koopman's theorem [61] for closed-shell compounds, η and μ can be calculated as

$$\eta = \frac{(I - A)}{2} \quad (2)$$

$$\mu = \frac{-(I + A)}{2} \quad (3)$$

where I and A are the ionization potential and electron affinity of the complexes, respectively. These parameters can be expressed through HOMO and LUMO orbital energies as $I = - E_{HOMO}$ and $A = - E_{LUMO}$.

$$S = \frac{1}{2\eta} \quad (4)$$

$$\omega = \frac{\mu^2}{2\eta} \quad (5)$$

Softness is a property of the molecule that measures the extent of chemical reactivity. It is the reciprocal of hardness. Moreover, the electrophilicity index determines the electrophilic nature of molecules. Finally, the molecular electrostatic potential (MEP) is utilized for interpreting and predicting the reactive behavior of the complexes in both electrophilic and nucleophilic attacks.

3. Results and discussion

3.1. Energies

According to Fig. 1, the cations (M = Li^+, Na^+, K^+, Mg^{2+}, and Ca^{2+}) are located on top of the plane of the aromatic ring in the studied complexes. The results propose that the binding strength depends on the nature of both the cation (radius and charge) and the π-system. The results of the BSSE-corrected binding energies (ΔE_{BSSE}) are collected in Table 1. As shown in this Table, the trend in ΔE_{BSSE} values for the ASA and TASA complexes is similar and obeys from π···Mg^{2+} > π···Ca^{2+} > π···Li^+ > π···Na^+ > π···K^+ order. This indicates that the ΔE_{BSSE} values enhance as the size of the cations reduces in each group. Comparing the ΔE_{BSSE} values with the charge-to-radius ratio of the cations shows a direct relationship between them as Mg^{2+} (3.077) > Ca^{2+} (2.020) > Li^+ (1.667) > Na^+ (1.052) > K^+ (0.752). As seen, the cations with higher charge density interact more strongly with the π-systems.

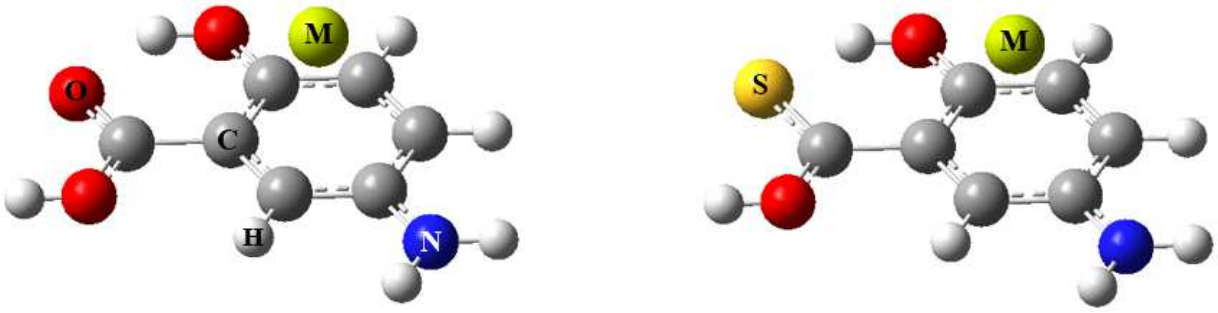

Fig. 1. Molecular structure of ASA···M (a) and TASA···M (b) complexes (M = Li^+, Na^+, K^+, Mg^{2+} and Ca^{2+}).

In the investigated complexes, the smaller radius and the more positive charge are related to the divalent cations compared to the monovalent ones. This leads to the transfer of a certain amount of the electron density from the quasi-ring created by the formation of O-H···O IMHB to the benzene ring. Thus, the more charge transfer from the benzene ring to the metal ions causes an increase in the cation–π interaction strength of divalent complexes. When the sulfur atom is replaced instead of oxygen, the ΔE_{BSSE} values increase for the divalent complexes, while the opposite trend is observed for the monovalent ones. The greater ion radius, the less positive charge, and the larger metal–benzene distance in the mono-charge cations relative to the double-charge ones lead to the weaker strength of cation–π interaction in these systems.

The HB energy (E_{HB}) is one of the most important aspects of hydrogen bonding systems. Various methods have been proposed to calculate the E_{HB}. The IMHB energies in the different configurations can be estimated by the Schuster method [62], related rotamers method (RRM) [63], and potential energy density method or Espinosa [64]. In this study, due to the interaction between different atoms in the investigated structures, it is not possible to accurately evaluate the hydrogen bond with the mentioned methods, so we use another method to calculate the E_{HB} of the analyzed complexes. The energy of a hydrogen bond can be estimated from the bond length using empirical relationships or theoretical models that relate the bond length and energy. One commonly used relationship is the linear correlation

between hydrogen bond energy and bond length proposed by Gavezzotti [65]:

$$E_{HB} = -16.8\ (1/r + 0.5d) \quad (6)$$

where E_{HB} is the hydrogen bond energy in kcal/mol, r is the hydrogen bond length in Å, and d is the sum of the van der Waals radii of the two atoms involved in the hydrogen bond. The term 0.5d accounts for the repulsive interactions between the atoms.

Based on the results obtained in Table 1, the replacement of O by S increases the HB energies in the related complexes. As shown in Table 1, the E_{HB} decreases in the following order: $\pi\cdots K^+ > \pi\cdots Na^+ > \pi\cdots Li^+ > \pi\cdots Ca^{2+} > \pi\cdots Mg^{2+}$, which has a reverse relationship with the ratio of charge-to-radius of the cations. The results also show that the presence of cation-π interaction decreases the E_{HB} strength in the divalent complexes, while the reverse process is observed in the monovalent ones. This result can be explained based on the charge values on the cations. Because the monovalent cations have less positive charge concerning divalent ones, the smaller charge density of these cations leads to the weaker strength of cation–π interaction; as a result, a negligible reduction occurs in the π-electron density of the HB quasi-ring. This increases the π-electron delocalization in the HB unit, which makes the HB strength stronger in these complexes. This indicates that for stronger HBs, the delocalization is more important than the electrostatic interaction energy, which may be a typical feature of HBs.

On the other hand, the strengthening of cation–π interactions in the divalent cations with the greater charge density may be due to the attraction effects between the cations and π-electrons of the ring that reduce the electron density within the HB quasi-ring and leads to weakening of the HB in these systems. From the calculated data, it can be concluded that the cation-π interactions in the monovalent complexes have a stronger influence on the HB strength with respect to those in the divalent complexes. However, the strongest cation-π interactions have the weakest HB strength and vice versa. As seen in Fig. 2, there are good linear correlations between the E_{HB} and ΔE_{BSSE} values in the studied complexes.

Table 1. The BSSE-corrected binding and IMHB energies (ΔE_{BSSE} and E_{HB}, in kcal mol^{-1}), the geometrical (bond lengths (d), in Å and bond angles (θ), in °) and spectroscopic descriptors (ν, in cm^{-1}) of complexes calculated at the ωB97XD/6-311++G(d,p) level of theory.

	ΔE_{BSSE}	$d_{\pi\cdots M}$	$\nu_{\pi\cdots M}$	E_{HB}	$d_{O\text{-}H}$	$d_{H\cdots O(S)}$	$\theta_{OHO(S)}$	$\nu_{O\text{-}H}$
ASA$\cdots Li^+$	-36.66	1.955	328.9	-32.207	0.976	1.795	141.6	3581.9
ASA$\cdots Na^+$	-24.75	2.500	191.2	-32.223	0.976	1.792	142.0	3591.5
ASA$\cdots K^+$	-18.89	2.890	115.7	-32.228	0.976	1.791	142.2	3591.9
ASA$\cdots Mg^{2+}$	-120.89	1.951	366.9	-32.130	0.981	1.810	138.6	3522.9
ASA$\cdots Ca^{2+}$	-87.51	2.331	295.7	-32.192	0.980	1.798	139.3	3529.7
TASA$\cdots Li^+$	-36.65	1.952	329.1	-33.258	0.982	2.085	148.7	3417.6
TASA$\cdots Na^+$	-24.64	2.496	197.0	-33.265	0.981	2.083	148.9	3433.7
TASA$\cdots K^+$	-18.83	2.883	121.3	-33.265	0.981	2.083	148.9	3447.8
TASA$\cdots Mg^{2+}$	-123.94	1.945	378.7	-33.162	0.987	2.110	146.7	3354.7
TASA$\cdots Ca^{2+}$	-89.83	2.324	311.8	-33.200	0.986	2.100	146.9	3360.7

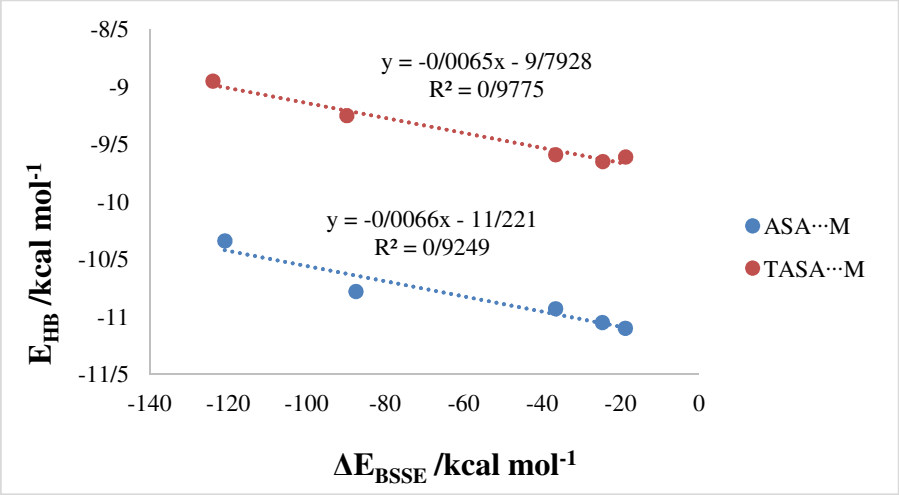

Fig. 2. The correlation between the E_{HB} and ΔE_{BSSE} values.

3.2. Molecular geometry

The most important structural parameter ($d_{\pi...M}$) for investigating the cation-π interaction is given in Table 1. In the selected complexes, the strength of the cation-π interaction is described by $d_{\pi...M}$ (the distance between the cation and the center of the aromatic ring). For each ion group (monovalent and divalent), a reverse relationship exists between the strength of cation-π interactions and the $d_{\pi...M}$ values. In other words, the stronger the binding energy ($|\Delta E_{BSSE}|$), the shorter the $d_{\pi...M}$. Based on the obtained data, the change of the $d_{\pi...M}$ in the different complexes depends on the type of cation. Inspection of results in Table 1 shows that the longest and shortest distances ($d_{\pi...M}$) are observed in the monovalent and divalent complexes, respectively. The substitution of O by S leads to a reduction in the $d_{\pi...M}$ values of the complexes. This means that the cation-π interactions in the TASA complexes are stronger than those of the ASA.

The strength of HB strongly changes with the structural parameters of the O–H···O(S) unit. The values obtained for the O–H bond length (d_{O-H}), H···O(S) distances ($d_{H...O(S)}$), and OHO(S) angles ($\theta_{OHO(S)}$) are listed in Table 1. Our data show that the increasing trend of $d_{H...O(S)}$ values is as $\pi\cdots Mg^{2+}$ > $\pi\cdots Ca^{2+}$ > $\pi\cdots Li^{+}$ > $\pi\cdots Na^{+}$ > $\pi\cdots K^{+}$ > ASA (or TASA). As shown in Table 1, in the presence of cation-π interaction, the values of d_{O-H} and $d_{H...O}$ decrease/increase, and the values of θ_{OHO} enhance/reduce for the monovalent/divalent complexes, respectively; this denotes that the strength of HB for the mentioned species becomes stronger/weaker, respectively. Similar results are also observed with the replacement of O by S in the studied complexes.

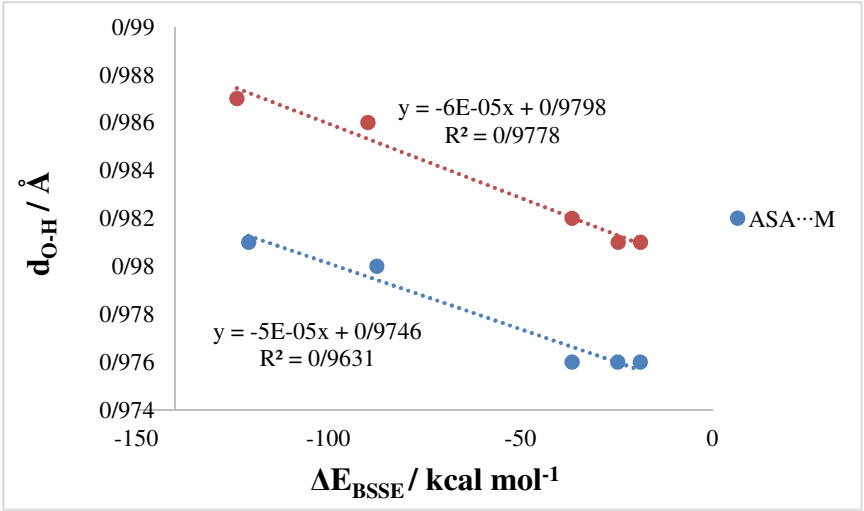

Fig. 3. The correlation between the d_{O-H} and ΔE_{BSSE} values.

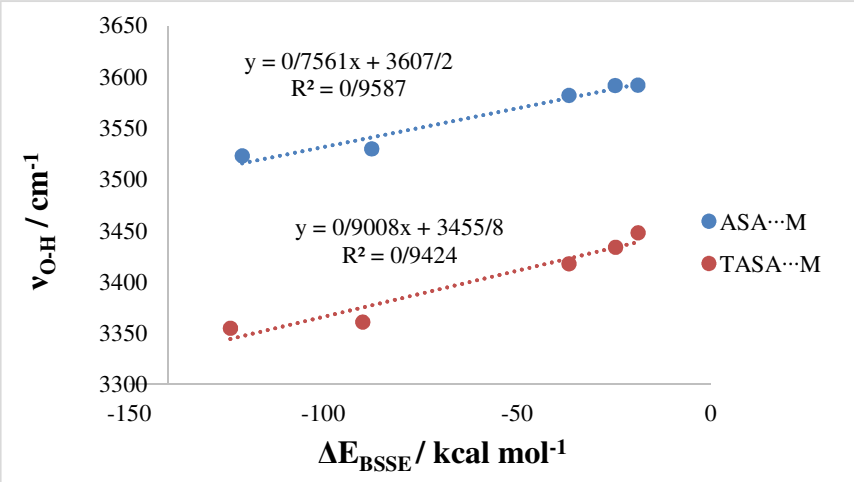

Fig. 4. The correlation between the $\nu_{O\text{-}H}$ and ΔE_{BSSE} values.

It is obvious from Table 1 that the simultaneous increase of the $d_{O\text{-}H}$ and $d_{H\cdots O(S)}$ in the complexes can be attributed to the electrostatic effects between the metal ions and the oxygen (or sulfur) atoms of the C=O(S) functional group connected to the phenyl ring. The existence of a negative charge on the oxygen (or sulfur) atoms causes these atoms to transfer a certain value of electron density to the metal ions, which makes the bonds longer in these complexes. Good relationships exist between the E_{HB} with values of $d_{H\cdots O}$ ($R^2 \approx 0.9971$) and $d_{H\cdots S}$ ($R^2 \approx 0.9935$), while there are less correlations among the E_{HB} with values of $d_{O\text{-}H}$ in the ASA ($R^2 \approx 0.8107$) and TASA ($R^2 \approx 0.9371$) complexes. Fig. 3 also illustrates the excellent linear correlations between the binding energies (ΔE_{BSSE}) and the $d_{O\text{-}H}$ values in the analyzed complexes.

3.3. Vibrational analysis

Another crucial aspect for evaluating the strength of cation-π interactions is the shift of the ion-π stretching frequencies ($\nu_{\pi\cdots M}$). Table 1 displays the values of $\nu_{\pi\cdots M}$ calculated for the complexes. There is a direct relationship between the strength of cation-π interactions and their corresponding stretching frequencies. In other words, the stronger the cation–π interaction, the larger the shifting. As shown in Table 1, the frequency values obtained in the divalent complexes are higher than the monovalent ones. A similar behavior is also observed with substituting S instead of O in the related complexes. However, the values of the stretching frequencies in the TASA complexes are larger than those in the ASA ones. This is in agreement with the greater binding energies (ΔE_{BSSE}) of these complexes in comparison with their corresponding values in the ASA species.

The HB strength can be described with the O-H stretching frequencies ($\nu_{O\text{–}H}$) in the O–H···O(S) unit. The results are given in Table 1. It is well-established that the strengthening of HB causes the frequency of O-H stretching mode to shift to lower frequencies. With the replacement of O by S, it is clear that the reduced values of $\nu_{O\text{–}H}$ in these complexes are in good accordance with their obtained E_{HBs}. In the conventional description of HB, the X–H···Y bond formation is associated with weakening and lengthening of the X–H covalent bond along with a decline in its stretching frequency [66]. The obtained data show that in the presence of cation-π interaction, the $\nu_{O\text{–}H}$ values of the monovalent complexes increase and those of the divalent structures decrease. This indicates an increment in the HB strength for the former cases and a reduction in that for the latter species. Similar results are also observed for the TASA complexes. Fig. 4 depicts the suitable linear relationships between the values of ΔE_{BSSE} and $\nu_{O\text{–}H}$ in the related complexes.

3.4. AIM analysis

In this section, the selected complexes are considered for the analysis of Bader's quantum theory of atoms in molecules (QTAIM) in terms of the electron density (ρ), its second derivative ($\nabla^2\rho$) at the bond critical point (BCP) and the total energy density (H) which is the sum of the kinetic energy density (G) and the potential energy density (V). The existence of cation-π interaction in the complexes is confirmed by the presence of a corresponding bond path in the electron density, which

is located between the cations and the carbon atoms of the ring. The number of BCPs changes with the type of cation and the nature of the π-system. As shown in Fig. 5, two BCPs, three-ring critical points (RCPs), and one cage critical point (CCP) are observed between the interacting cations with the benzene ring.

The topological descriptors of AIM analysis are given in Table 2. One of the appropriate parameters for describing the strength of ion–π interactions is the electron density [67]. The results of Table 2 show that the trend in the $\rho(r)_{\pi\cdots M}$ values is as $\pi\cdots Mg^{2+} > \pi\cdots Ca^{2+} > \pi\cdots Li^{+} > \pi\cdots Na^{+} > \pi\cdots K^{+}$. As seen, the order of the calculated $\rho(r)_{\pi\cdots M}$ values is similar to the values of ΔE_{BSSE} obtained at the ωB97XD/6-311++G(d,p) level of theory (see Tables 1 and 2). The linear correlation coefficients (R^2) for the dependence between the $\rho(r)_{\pi\cdots M}$ and ΔE_{BSSE} values in the ASA and TASA complexes are equal to 0.9820 and 0.9773, respectively. Our data also display that the substitution of O by S increases the $\rho(r)_{\pi\cdots M}$ values of the complexes.

For the analyzed systems, the values of $\nabla^2\rho(r)_{\pi\cdots M}$ and $H(r)_{\pi\cdots M}$ are found to be positive. This indicates the presence of closed-shell interactions in these complexes. By using the negative ratio of Hamiltonian components (−G/V), the characteristics of NCIs can also be explored [68, 69]. The covalent interactions show −G/V = 0; for the partially covalent interactions, the value of −G/V is between 0.5 and 1 (0.5 < −G/V < 1), and also for the electrostatic interactions, −G/V ≥ 1. As observed in Table 2, the calculated values of $-G/V_{\pi\cdots M}$ for all complexes belong to the electrostatic interactions.

The results of AIM analysis for BCPs of HB are listed in Table 2. In most cases, comparing the electron density at $\rho(r)_{H\cdots O(S)}$ with the HB energies shows a good relationship between them [70]. The results of Table 2 show that the trend in ($\rho(r)_{H\cdots O}$) values is as $ASA\cdots Ca^{2+}$ (0.0374) > $ASA\cdots Mg^{2+}$ (0.0363) and $ASA\cdots K^{+}$ (0.0381) > $ASA\cdots Na^{+}$ (0.0379) > $ASA\cdots Li^{+}$ (0.0377 a.u.), which is in agreement with the values of $d_{H\ldots O}$. The presence of cation-π interaction decreases the $\rho(r)_{H\cdots O}$ values of the divalent complexes compared to the monovalent ones, which suggests a weaker HB interaction in the former cases relative to the latter. Similar to the ASA complexes, it is also found that the replacement of O by S increases the $\rho(r)_{H\cdots S}$ values of the single-charge complexes, while for the double-charge species, the reverse process is observed.

For the analyzed complexes, good linear relationships can be observed among the $\rho(r)_{H\cdots O(S)}$ and ΔE_{BSSE} values with correlation coefficients (R^2) equal to 0.8981 (ASA) and 0.9611 (TASA) (see Fig. 6). Our findings also display that all complexes are placed in the medium HBs category; because all the bonds show $\nabla^2\rho(r)_{H\cdots O(S)} > 0$ and $H(r)_{H\cdots O(S)} < 0$ (see Table 2). According to the calculated results, the obtained values of $-G/V_{H\cdots O(S)}$ indicate the partially covalent nature of the HB interactions. However, the effects of substitution of O by S in the selected complexes denote increasing the covalent nature of HBs.

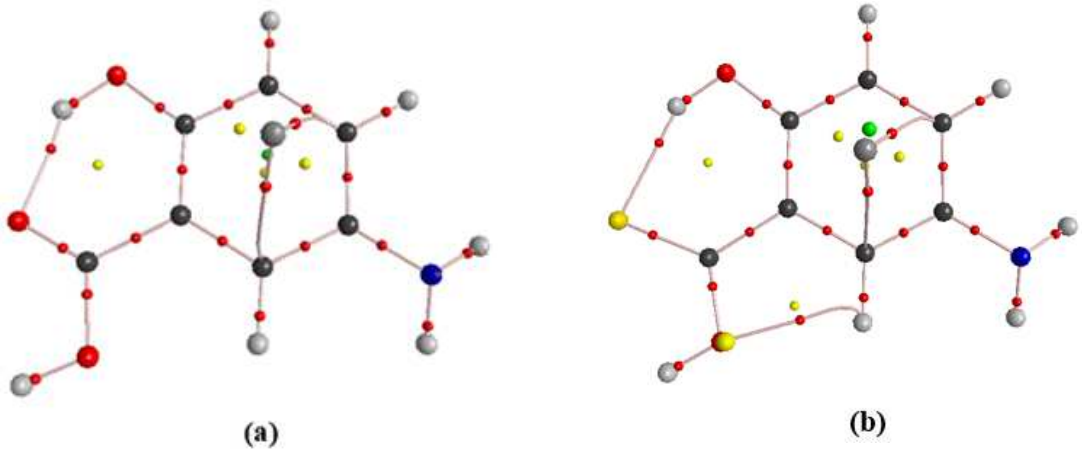

Fig. 5. Typical molecular graphs obtained from AIM analysis for ASA···M (a) and TASA···M (b) complexes. The small red, yellow, green spheres, and lines correspond to bond critical points (BCPs), ring critical points (RCPs), cage critical point (CCP) and bond paths, respectively.

Table 2. The selected topological properties of electron density (a.u.) obtained by AIM analysis.

	π···M					HB				
	ρ(r)	$\nabla^2\rho(r)$	H(r)	V(r)	-G/V	ρ(r)	$\nabla^2\rho(r)$	H(r)	V(r)	-G/V
ASA···Li^+	0.0147	0.0775	0.0039	-0.0115	1.342	0.0377	0.1260	-0.0016	-0.0348	0.953
ASA···Na^+	0.0097	0.0451	0.0025	-0.0062	1.404	0.0379	0.1269	-0.0017	-0.0352	0.951
ASA···K^+	0.0096	0.0374	0.0019	-0.0057	1.328	0.0381	0.1274	-0.0018	-0.0354	0.950
ASA···Mg^{2+}	0.0298	0.1253	0.0027	-0.0259	1.104	0.0363	0.1211	-0.0013	-0.0329	0.960
ASA···Ca^{2+}	0.0253	0.0866	0.0013	-0.0190	1.070	0.0374	0.1241	-0.0017	-0.0343	0.952
TASA···Li^+	0.0153	0.0805	0.0040	-0.0121	1.331	0.0384	0.0650	-0.0071	-0.0305	0.766
TASA···Na^+	0.0098	0.0467	0.0026	-0.0065	1.402	0.0386	0.0655	-0.0072	-0.0307	0.766
TASA···K^+	0.0097	0.0368	0.0018	-0.0056	1.324	0.0384	0.0658	-0.0071	-0.0306	0.769
TASA···Mg^{2+}	0.0312	0.1390	0.0027	-0.0293	1.092	0.0368	0.0615	-0.0066	-0.0285	0.770
TASA···Ca^{2+}	0.0269	0.0907	0.0006	-0.0215	1.028	0.0376	0.0625	-0.0069	-0.0295	0.765

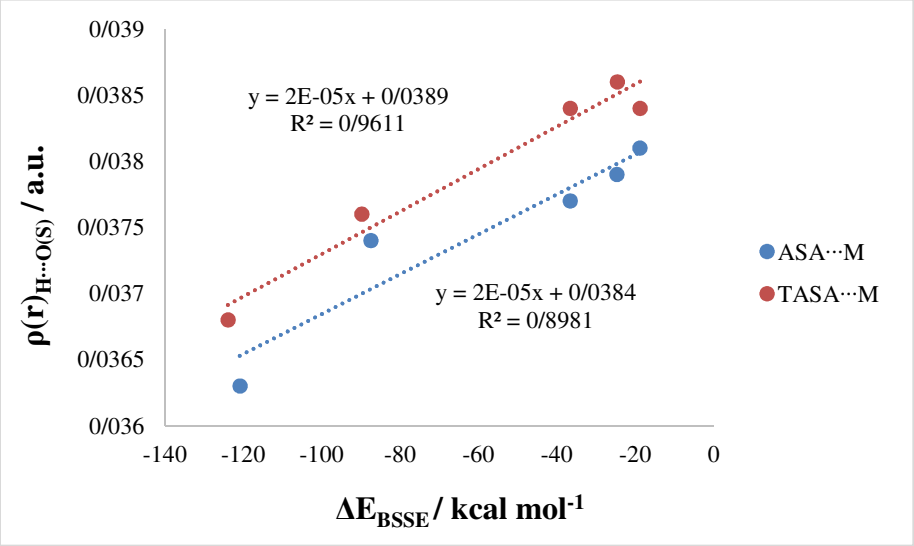

Fig. 6. Correlation between the ΔE_{BSSE} and $\rho(r)_{H\cdots O(S)}$ values.

3.5. NBO analysis

The electron populations obtained from the NBO analysis [56] give insight into the electronic nature of the complexes. The theoretical results show that the $\sigma_{(C=C)} \rightarrow LP^*_{(M)}$ interaction is the most important among the studied structures. Herein, the charge is transferred from the π-systems toward the cations. In other words, $\sigma_{(C=C)}$ of the aromatic ring and the $LP^*_{(M)}$ participate as donors and acceptors, respectively. The results of NBO analysis are collected in Table 3. As shown in this Table, the trend in $E^{(2)}$ values is as $\pi\cdots Mg^{2+} > \pi\cdots Ca^{2+} > \pi\cdots Li^+ > \pi\cdots Na^+ > \pi\cdots K^+$, which is directly proportional to the calculated $\rho(r)_{\pi\cdots M}$ values. There are also good linear relationships between the ΔE_{BSSE} and the $E^{(2)}$ values. The correlation coefficients for ASA and TASA

complexes are equal to 0.9206 and 0.9462, respectively. The theoretical results reveal that the substitution of O by S increases the $E^{(2)}$ values in the studied complexes so that these values are higher in the divalent complexes relative to the monovalent ones.

From the atomic charge difference of the free cation and the complex, the amount of charge transfer ($\Delta q_{(CT1)}$) between the aromatic ring and the cations is estimated. The results are given in Table 3. As seen in this Table, the ($\Delta q_{(CT1)}$) values in the TASA complexes are higher than the ASA ones. Moreover, our findings show that these values are the highest for the double-charge complexes, while the lowest values belong to the mono-charge ones. It is obvious from Table 3 that the trend in the $\Delta q_{(CT1)}$ values is identical with the $E^{(2)}$ values.

The results of NBO analysis corresponding to HB are listed in Table 3. The computations show that the most significant donor–acceptor interaction in the analyzed complexes is $LP_{O(S)} \rightarrow \sigma^*_{(O-H)}$. As shown in Table 3, the simultaneous presence of the HB and cation–π interactions increases the HB strength for monovalent complexes, while this merging has the opposite effect on the HB of divalent complexes. Similar results have also been obtained for the TASA complexes. Furthermore, the correlation coefficients of 0.9667 and 0.8051 indicate reasonable linear relationships between the values of ΔE_{BSSE} and $E^{(2)}$ corresponding to HB for the ASA and TASA complexes, respectively (see Fig. 7).

Table 3 shows the values of the charge transfer ($\Delta q_{(CT2)}$) related to the HB. The values of $\Delta q_{(CT2)}$ can be evaluated with an equation as $\Delta q_{(CT2)} = q_{O(S)}$ (complex) - $q_{O(S)}$ (monomer). According to this formula, $q_{O(S)}$ (complex) is the atomic charge of the oxygen (or sulfur) involved in HB, and $q_{O(S)}$ (monomer) is the charge of the oxygen (or sulfur) atom in its equivalent monomer (q_O = -0.344 and q_S = -0.704). As seen in Table 3, the most negative atomic charges ($q_{O(S)}$) belong to the monovalent complexes, while the least of those are related to the divalent ones. It is also apparent from Table 3 that the presence of cation-π interaction increases/decreases the values of $\Delta q_{(CT2)}$ for the divalent/monovalent complexes, respectively. This means that the charge transfer may be a helpful feature for depicting the strength of these interactions.

Table 3. The values of $E^{(2)}$ correspond to $\sigma_{(C=C)} \rightarrow LP^*_{(M)}$ and $LP_{O(S)} \rightarrow \sigma^*_{(O-H)}$ interactions (in kcalmol^{-1}), occupation numbers of donor (ON_D) and acceptor (ON_A) orbitals, charge density on oxygen (sulfur) atom ($q_{O(S)}$, in e) and the charge transfers ($\Delta q_{(CT)}$ in e) in the studied complexes.

	π···M interaction				HB interaction				
	$\sigma_{(C=C)} \rightarrow LP^*_{(M)}$				$LP_{O(S)} \rightarrow \sigma^*_{(O-H)}$				
	$E^{(2)}$	$ON_{\pi(C=C)}$	$ON_{LP^*(M)}$	$\Delta q_{(CT1)}$	$E^{(2)}$	$ON_{LPO(S)}$	$ON_{\sigma^*(O-H)}$	$q_{O(S)}$	$\Delta q_{(CT2)}$
ASA···Li^+	1.25	1.974	0.028	0.373	13.49	1.847	0.036	-0.271	0.073
ASA···Na^+	1.21	1.977	0.014	0.147	13.66	1.849	0.036	-0.284	0.060
ASA···K^+	1.13	1.972	0.009	0.019	13.77	1.850	0.036	-0.292	0.052
ASA···Mg^{2+}	3.03	1.970	0.010	1.062	12.33	1.838	0.035	-0.215	0.129
ASA···Ca^{2+}	1.42	1.973	0.010	0.535	13.05	1.841	0.036	-0.231	0.113
TASA···Li^+	1.37	1.977	0.020	0.392	30.38	1.821	0.081	-0.567	0.137
TASA···Na^+	1.31	1.978	0.014	0.159	30.27	1.824	0.081	-0.599	0.105
TASA···K^+	1.25	1.971	0.010	0.026	29.86	1.826	0.080	-0.614	0.090
TASA···Mg^{2+}	3.20	1.966	0.010	1.081	28.38	1.803	0.082	-0.318	0.386
TASA···Ca^{2+}	1.53	1.969	0.010	0.554	29.51	1.807	0.083	-0.348	0.356

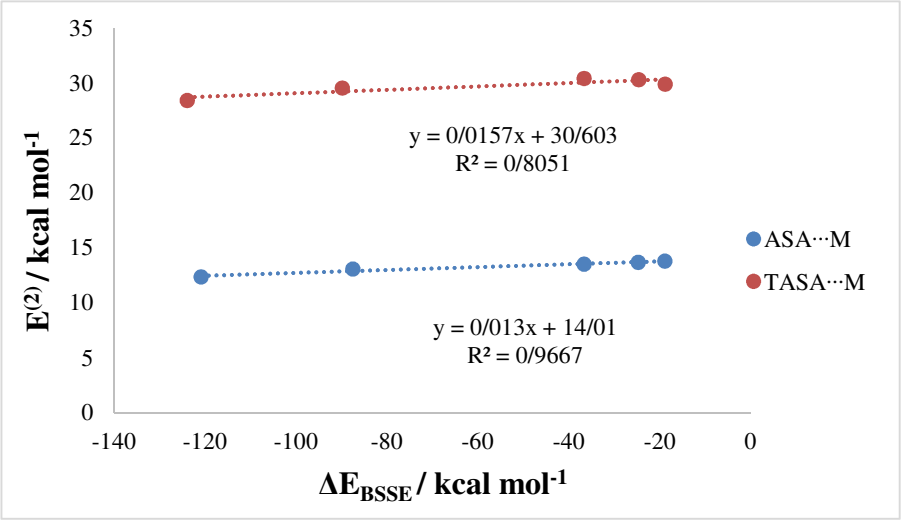

Fig. 7. Correlation between the ΔE_{BSSE} and the $E^{(2)}$ corresponding to HB.

3.6. HOMO-LUMO analysis

The energy gap (E_g) between the highest occupied molecular orbital (HOMO) and the lowest unoccupied molecular orbital (LUMO) reveals the molecular electrical transport properties. The E_g is determined from the energy difference between the HOMO and LUMO as follows: $E_g = E_{LUMO} - E_{HOMO}$. The E_{HOMO} is the energy of the Fermi level and the E_{LUMO} is the first eigenvalue of the valance band. The HOMO and LUMO plots of the ASA···Li^+ and TASA···Li^+ complexes calculated at the ωB97XD/6-311++G(d,p) level of theory are illustrated in Fig. 8. The DFT-based reactivity and stability descriptors of complexes such as chemical hardness (η), chemical softness (S), electronic chemical potential (μ), electronegativity (χ) and electrophilicity index (ω) are obtained using the molecular orbital energy values (see Table 4).

It is well known that the complexes having the large E_g are hard and the complexes having the small E_g are soft. Our findings show that the maximum and minimum values of η correspond to the Li^+ and Mg^{2+} complexes, respectively. Therefore, the Li^+ complexes with the larger E_g are more stable and harder, while the Mg^{2+} complexes with the lower E_g are more reactive and thus softer. Hence, the simultaneous presence of the HB and cation–π interactions leads to the high chemical stability and the low chemical reactivity of the ASA complexes. This result is due to the increase in η and also a decrease in S of complexes in the present study. The reverse results are observed for the TASA complexes.

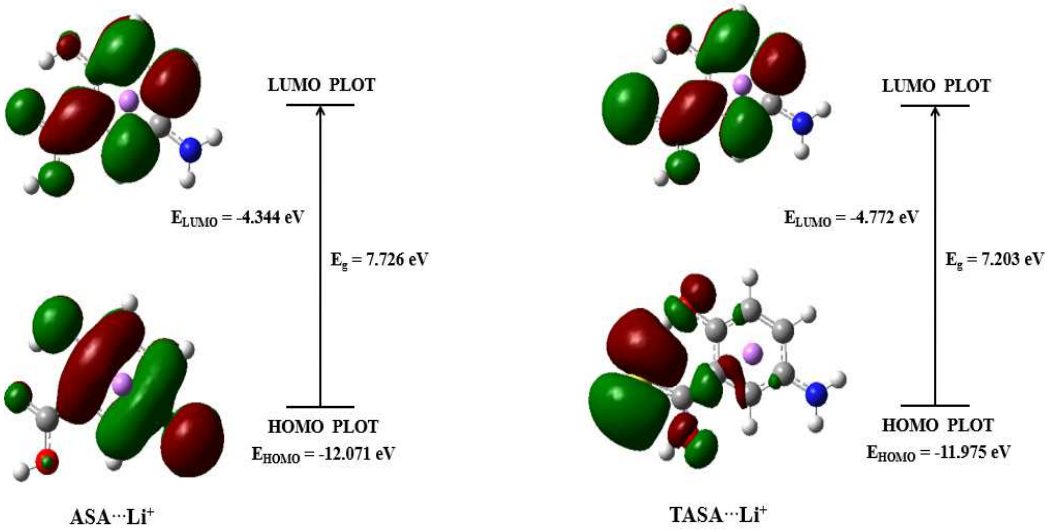

Fig. 8. The HOMO and LUMO of ASA···Li^+ and TASA···Li^+ complexes.

The results obtained in Table 4 also indicate that all the selected complexes are stable due to their negative electronic chemical potentials. There is a meaningful relationship between the values of electronegativity and the chemical potential as $\chi = -\mu$. As observed in Table 4, the best electron acceptors belong to the divalent complexes; because they have the highest electronegativity values. The electrophilicity index is another powerful tool for studying the reactivity of complexes. According to the electrophilic nature of molecules, the electrophilicity index (ω) is categorized as the weak electrophiles ($\omega < 0.8$ eV), the medium electrophiles ($0.8 < \omega < 1.5$ eV) and the strong electrophiles ($\omega > 1.5$ eV) [71]. Our results confirm that the studied complexes are placed in the strong electrophiles category. In addition, the obtained data show the most/least values of electrophilicity for the divalent/monovalent complexes, respectively.

Table 4. Values of the HOMO and LUMO energies (E_{HOMO} and E_{LUMO}), energy gap (E_g), chemical hardness (η), softness (S), electronic chemical potential (μ), electronegativity (χ) and electrophilicity index (ω).

	E_{HOMO} (eV)	E_{LUMO} (eV)	E_g (eV)	η (eV)	S (eV^{-1})	μ (eV)	χ (eV)	ω (eV)
ASA···Li^+	-12.071	-4.344	7.726	3.863	0.129	-8.208	8.208	8.719
ASA···Na^+	-11.618	-3.910	7.708	3.854	0.130	-7.764	7.764	7.821
ASA···K^+	-11.377	-3.658	7.719	3.859	0.130	-7.517	7.517	7.322
ASA···Mg^{2+}	-16.586	-10.110	6.478	3.239	0.154	-13.347	13.347	27.497
ASA···Ca^{2+}	-16.109	-8.952	7.157	3.578	0.140	-12.530	12.530	21.939
TASA···Li^+	-11.975	-4.772	7.203	3.601	0.139	-8.374	8.374	9.735
TASA···Na^+	-11.547	-4.413	7.134	3.567	0.140	-7.980	7.980	8.927
TASA···K^+	-11.315	-4.202	7.113	3.556	0.141	-7.758	7.758	8.462
TASA···Mg^{2+}	-16.252	-9.942	6.310	3.155	0.158	-13.097	13.097	27.183
TASA···Ca^{2+}	-15.891	-8.946	6.945	3.472	0.144	-12.419	12.419	22.207

3.7. Molecular electrostatic potential

The size, shape, and charge distribution in the molecules can be visualized by molecular electrostatic potential (MEP) maps. The values of surface electrostatic potentials are shown in different colors. The most negative site belongs to the red color, while the most positive site corresponds to the blue color [72-75]. The green color represents areas with zero potential. The regions of attractive potential participate in the nucleophilic reactions, while the regions of repulsive potential contribute to the electrophilic attacks.

The electron density isosurfaces for the ASA···Li^+ and TASA···Li^+ complexes calculated by ωB97XD method and 6-311++G(d,p) basis set are illustrated in Fig. 9. As observed in this Figure, the negative charge is covered with the oxygen atoms of OH and COOH functional groups (red and yellow colors), which have the greater electronegativity and the higher electron density. This provides the most electrophilic region in the complexes. On the other hand, the positive region is over the Li^+ cation and the plane of the aromatic ring (blue color), which supports the most nucleophilic region in the complexes.

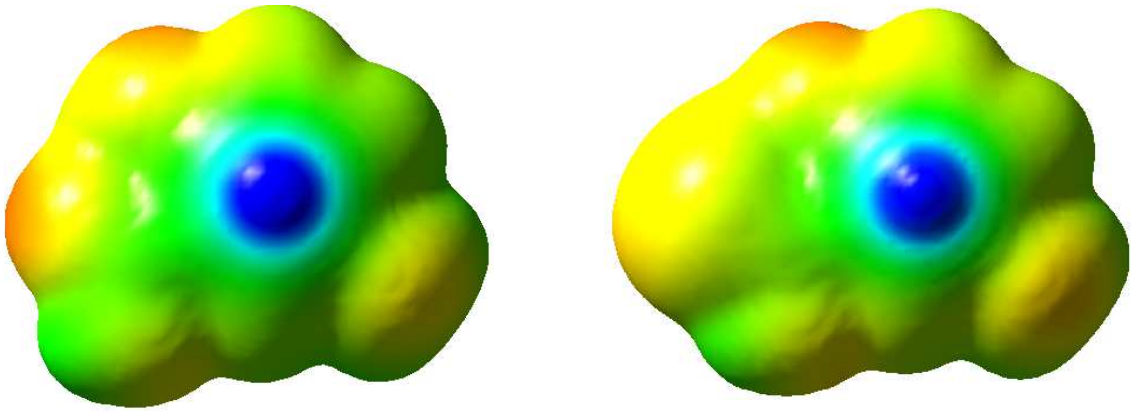

ASA···Li$^+$ **TASA···Li$^+$**

Fig. 9. Electron density isosurfaces for ASA···Li$^+$ and TASA···Li$^+$ complexes calculated by ωB97XD method and 6-311++G(d,p) basis set.

4. Conclusions

In the present study, the NCIs are investigated on the complexes of ASA and its thio analogous (TASA) at the ωB97XD/6-311++G(d,p) level of theory. The results show that the replacement of O by S enhances the E_{HB} strength in the complexes. On the other hand, the presence of cation-π interaction increases the HB energies in the monovalent complexes, while the reverse process is observed for the divalent ones. As a result, the cation-π interactions in the monovalent complexes have a stronger influence on the HB strength with respect to those in the divalent complexes. These results are also confirmed by the AIM analysis. For the studied systems, the values of $\nabla^2\rho(r)_{\pi\cdots M}$ and $H(r)_{\pi\cdots M}$ are positive. This indicates the presence of closed-shell interactions in these complexes. Our findings also display that all species are placed in the medium HBs category. The results of NBO analysis show that the values of charge transfer are the highest for the divalent complexes, while the lowest values belong to the monovalent ones. Based on the molecular orbital data, the Li^+ complexes with the larger energy gap are more stable and harder, while the Mg^{2+} complexes with the lower energy gap are more reactive and thus softer. The simultaneous presence of the HB and cation–π interactions leads to the high chemical stability in the ASA complexes and the high chemical reactivity in the TASA species.

Acknowledgements

The authors wish to thank the Payame Noor University, Tehran, Iran for its support.

References

[1] C. Stolfi, V. De Simone, F. Pallone, G. Monteleone, Mechanisms of action of non-steroidal anti-inflammatory drugs (NSAIDs) and mesalazine in the chemoprevention of colorectal cancer. *Int. J. Mol. Sci.*, 14(9) (2013) 17972.

[2] J. Mayberry, The history of 5-ASA compounds and their use in ulcerative colitis-trailblazing discoveries in gastroenterology. *J. Gastrointestin. Liver Dis.*, 22(4) (2013) 375.

[3] C. T. Xu, S. Y. Meng, B. R. Pan, Drug therapy for ulcerative colitis. *World J. Gastroenterol.*, 10(16) (2004) 2311.

[4] Y. Cheng, P. Desreumaux, 5-aminosalicylic acid is an attractive candidate agent for chemoprevention of colon cancer in patients with inflammatory bowel disease. *World J. Gastroenterol.*, 11(3) (2005) 309.

[5] O. H. Nielsen, I. Ahnfelt-Rønne, J. Elmgreen, Abnormal metabolism of arachidonic acid in chronic inflammatory bowel disease: enhanced release of leukotriene B4 from activated neutrophils. *Gut.*, 28(2) (1987) 181.

[6] S. Sule, A. Rosen, M. Petri, E. Akhter, F. Andrade, Abnormal production of pro- and anti-inflammatory cytokines by lupus monocytes in response to apoptotic cells. *PLOS One*, 6(3) (2011) e17495.

[7] P. Hubza, K. Moller-Dethlefs, Non-covalent interactions: Theory and experiment, Royal society of chemistry, Cambridge (2010).

[8] S. Scheiner, Non-covalent forces, Springer, Heidelberg (2015).

[9] S. J. Grabowski, Hydrogen bonding – New insights, Springer, Berlin (2006).

[10] G. R. Desiraju, T. Steiner, The weak hydrogen bond in structural chemistry and biology, Oxford university press, Oxford (2001).

[11] G.A. Jeffrey, An introduction to hydrogen bonding, Oxford University Press, New York (1997).
[12] G.R. Desiraju, Hydrogen bridges in crystal engineering: interactions without borders. *Acc. Chem. Res.,* 35 (2002) 565.
[13] H. Raissi, A. Khanmohammadi, F. Mollania, A theoretical DFT study on the structural parameters and intramolecular hydrogen-bond strength in substituted (Z)-N(Thionitrosomethylene)-thiohydroxylamine systems. *Bull. Chem. Soc. Jpn.,* 86 (2013) 1261.
[14] L. Hokmabady, H. Raissi, A. Khanmohammadi, Interactions of the 5-fluorouracil anticancer drug with DNA pyrimidine bases: a detailed computational approach. *Struct. Chem.,* 27 (2016) 487.
[15] H. Umeyama, K. Morokuma, The origin of hydrogen bonding. An energy decomposition study. *J. Am. Chem. Soc.,* 99 (1977) 1316.
[16] J. P. Foster, F. Weinhold, Natural hybrid orbitals. *J. Am. Chem. Soc.,* 102 (1980) 7211.
[17] E. D. Glendening, A. Streitwieser, Natural energy decomposition analysis: An energy partitioning procedure for molecular interactions with application to weak hydrogen bonding, strong ionic, and moderate donor–acceptor interactions. *J. Chem. Phys.,* 100 (1994) 2900.
[18] B. Jeziorski, R. Moszyński, K. Szalewicz, Perturbation Theory Approach to Intermolecular Potential Energy Surfaces of van der Waals Complexes. *Chem. Rev.,* 94 (1994) 1887.
[19] A. Khanmohammadi, H. Raissi, F. Mollania, L. Hokmabadi, Molecular structure and bonding character of mono and divalent metal cations (Li^+, Na^+, K^+, Be^{2+}, Mg^{2+}, and Ca^{2+}) with substituted benzene derivatives: AIM, NBO, and NMR analyses. *Struct. Chem.,* 25 (2014) 1327.
[20] M. Mohammadi, M. Mahinian, A. Khanmohammadi, Theoretical study of stability and electronic characteristics in various complexes of psoralen as an anticancer drug in gas phase, water and CCl_4 solutions. *Chem. Res. Chin. Univ.,* 38(6) (2022) 1414.
[21] A. Hassanpour, M. R. Poor Heravi, A. Khanmohammadi, Electronic sensors for alkali and alkaline earth cations based on Fullerene-C60 and silicon doped on C60 nanocages: a computational study. *J. Mol. Model.,* 28 (2022) 148.
[22] M. Mohammadi, A. Khanmohammadi, Molecular structure, QTAIM and bonding character of cation–π interactions of mono- and divalent metal cations (Li^+, Na^+, K^+, Be^{2+}, Mg^{2+} and Ca^{2+}) with drug of acetaminophen. *Theor. Chem. Acc.,* 138 (2019) 101.
[23] F. Alirezapour, A. Khanmohammadi, Theoretical study on the interaction of phenylalaninal with group IA (Li^+, Na^+, K^+) and IIA (Be^{2+}, Mg^{2+}, Ca^{2+}) metal cations. *J. Chin. Chem. Soc.,* 68 (2021) 1002.
[24] F. Alirezapour, A. Khanmohammadi, The effect of cation–π interactions on the stability and electronic properties of anticancer drug Altretamine: a theoretical study. *Acta Cryst.,* C76 (2020) 982.
[25] R. Bhattacharyya, U. Samanta, P. Chakrabarti, Aromatic–aromatic interactions in and around α-helices. *Protein Eng. Des. Sel.*, 15 (2002) 91.
[26] R. Kumpf, D. Dougherty, A Mechanism for Ion Selectivity in Potassium Channels: Computational Studies of Cation-π Interactions. *Science*, 261 (1993) 1708.
[27] A. S. Mahadevi, G. N. Sastry, Cation-π Interaction: Its Role and Relevance in Chemistry, Biology, and Material Science. *Chem. Rev.*, 113 (2013) 2100.
[28] V. Percec, M. Glodde, T. K. Bera, Y. Miura, I. Shiyanovskaya, K. D. Singer, V. S. K. Balagurusamy, P. A. Heiney, I. Schnell, A. Rapp, H. W. Spiess, S. D. Hudson, H. Duan, Self-organization of supramolecular helical dendrimers into complex electronic materials. *Nature*, 419 (2002) 384.
[29] L. Zang, Y. Che, J. S. Moore, One-Dimensional Self-Assembly of Planar π-Conjugated Molecules: Adaptable Building Blocks for Organic Nanodevices. *Acc. Chem. Res.*, 41 (2008) 1596.
[30] C. D. Sherrill, Energy Component Analysis of π Interactions. *Acc. Chem. Res.*, 46 (2013) 1020.
[31] N. J. Singh, S. K. Min, D. Y. Kim, K. S. Kim, Comprehensive Energy Analysis for Various Types of π-Interaction. *J. Chem. Theory Comput.*, 5 (2009) 515.
[32] W. Wang, Y. Zhang, K. Huang, Unconventional interaction in N(P)-related systems. *Chem. Phys. Lett.*, 411 (2005) 439.
[33] M. Mohammadi, F. Hoseinpour, A. Khanmohammadi, A DFT theoretical investigation on the interplay effects between cation-π and intramolecular hydrogen bond interactions in the mesalazine···Fe^{2+} binary complex. *Theor. Chem. Acc.*, 141 (2022) 38.
[34] M. Mohammadi, F. Alirezapour, A. Khanmohammadi, DFT calculation of the interplay effects between cation–π and intramolecular hydrogen bond interactions of mesalazine drug with selected transition metal ions (Mn^+, Fe^{2+}, Co^+, Ni^{2+}, Cu^+, Zn^{2+}). *Theor. Chem. Acc.,* 140 (2021) 104.
[35] M. Pirgheibi, M. Mohammadi, A. Khanmohammadi, A comparative study of interplay effects between the cation-π and intramolecular hydrogen bond interactions in the various complexes of methyl salicylate with Mn^+, Fe^{2+}, Co^+, Ni^{2+}, Cu^+, and Zn^{2+} cations. *Struct. Chem.,* 32 (2021) 1529.
[36] F. Alirezapour, A. Khanmohammadi, Computational study of noncovalent interactions within the various complexes of para aminosalicylic acid and Cr^{2+}, Mn^+, Fe^{2+}, Co^+, Ni^{2+}, Cu^+, Zn^{2+} cations: exploration of the enhancing effect of the cation–π interaction on the intramolecular hydrogen bond. *Theor. Chem. Acc.,* 139 (2020) 180.
[37] A. Siadati, A theoretical study on the possibility of functionalization of C20 fullerene via its Diels-Alder reaction with 1, 3-butadiene. *Lett. Org. Chem.,* 13(1) (2016) 2.

[38] S. A. Siadati, Effect of steric congestion on the stepwise character and synchronicity of a 1, 3-dipolar reaction of a nitrile ylide and an olefin. *J. Chem. Res.,* 39(11) (2015) 640.

[39] A. R. Bekhradnia, S. Arshadi, S. A. Siadati, 1, 3-Dipolar cycloaddition between substituted phenyl azide and 2, 3-dihydrofuran. *Chem. Pap.,* 68 (2014) 283.

[40] F. Alirezapour, M. Mohammadi, A. Khanmohammadi, Exploration of the mutual effects between cation–π and intramolecular hydrogen bond interactions in the different complexes of mesalazine with metal cations of alkali and alkaline-earth: A DFT study. *Chem. Rev. Lett.*, 6 (2023) 262.

[41] M. Javdani Zamani Sagheb, L. Hokmabady, A. Khanmohammadi, A comprehensive investigation into the effect of substitution on electronic structure, charge transfer, resonance, and strength of hydrogen bond in 3–amino-propene thial and its analogous: A DFT calculation. *Chem. Rev. Lett.*, 6 (2023) 308.

[42] I. Sabeeh Hasan, A. Arkan Majhool, M. Humam Sami, M. Adil, S. Salbiah Syed Abdul Azziz, DFT Investigation of Structure, stability, NBO charge on Titanium-Nitrogen Nanoheterofullerenes evolved from a small nanocage. *Chem. Rev. Lett.*, 6 (2023) 297.

[43] A. Jimoh, E. B. Agbaji, V. O. Ajibola, S. Uba, Optimization of the production of Methyl Ester from used cotton Seed Oil: A Statistical Approach using box-behnken design. *Chem. Rev. Lett.*, 6 (2023) 183.

[44] M. Pirgheibi, M. Mohammadi, A. Khanmohammadi, Density functional theory study of the interplay between cation–π and intramolecular hydrogen bonding interactions in complexes involving methyl salicylate with Li^+, Na^+, K^+, Be^{2+}, Mg^{2+}, Ca^{2+} cations. *Comput. Theor. Chem.*, 1198 (2021) 113172.

[45] M. Mohammadi, A. Khanmohammadi, Theoretical investigation on the non-covalent interactions of acetaminophen complex in different solvents: study of the enhancing effect of the cation–π interaction on the intramolecular hydrogen bond. *Theor. Chem. Acc.*, 139 (2020) 141.

[46] A. Khanmohammadi, F. Ravari, The influence of cation-π interactions on the strength and nature of intramolecular O¨¨H hydrogen bond in orthohydroxy benzaldehyde compound. *Phys. Chem. Res.*, 5 (2017) 57.

[47] J. S. Rao, H. Zipse, G. N. Sastry, Explicit solvent effect on cation-π interactions: a first principle investigation. *J. Phys. Chem. B*, 113 (2009) 7225.

[48] (a) J. Munoz, J. Sponer, P. Hobza, M. Orozco, F. J. Luque, Interactions of Hydrated Mg^{2+} Cation with Bases, Base Pairs, and Nucleotides. Electron Topology, Natural Bond Orbital, Electrostatic, and Vibrational Study. *J. Phys. Chem. B*, 105 (2001) 6051. (b) J. Gu, J. Leszczynski, A Theoretical Study of Thymine and Uracil Tetrads: Structures, Properties, and Interactions with the Monovalent K^+ Cation. *J. Phys. Chem. A*, 105 (2001) 10366.

[49] A. M. Pyle, Metal ions in the structure and function of RNA. *J. Biol. Inorg. Chem.*, 7 (2002) 679.

[50] J. D. Chai, M. Head-Gordon, Long-range corrected hybrid density functionals with damped atom–atom dispersion corrections. *Phys. Chem. Chem. Phys.*, 10 (2008) 6615.

[51] R. Krishnam, J. S. Binkley, R. Seeger, J. A. Pople, Self- consistent molecular orbital methods 25. Supplementary functions for Gaussian basis sets. *J. Chem. Phys.*, 80 (1984) 3265.

[52] M. J. Frisch, G. W. Trucks, H. B. Schlegel, G. E. Scuseria, M. A. Robb, J. R. Cheese-man, G. Scalmani, V. Barone, B. Mennucci, G. A. Petersson, H. Nakatsuji, M. Caricato, X. Li, H. P. Hratchian, A. F. Izmaylov, J. Bloino, G. Zheng, J. L. Son-nenberg, M. Hada, M. Ehara, K. Toyota, R. Fukuda, J. Hasegawa, M. Ishida, T. Nakajima, Y. Honda, O. Kitao, H. Nakai, T. Vreven, J. A. Montgomery Jr, J. E. Peralta, F. Ogliaro, M. J. Bearpark, J. Heyd, E. N. Brothers, K. N. Kudin, V. N. Staroverov, R. Kobayashi, J. Normand, K. Raghavachari, A. P. Rendell, J. C. Bu-rant, S. S. Iyengar, J. Tomasi, M. Cossi, N. Rega, N. J. Millam, M. Klene, J. E. Knox, J. B. Cross, V. Bakken, C. Adamo, J. Jaramillo, R. Gomperts, R. E. Stratmann, O. Yazyev, A. J. Austin, R. Cammi, C. Pomelli, J. W. Ochterski, R. L. Martin, K. Mo-rokuma, V. G. Zakrzewski, G. A. Voth, P. Salvador, J. J. Dannenberg, S. Dapprich, A. D. Daniels, Ö. Farkas, J. B. Foresman, J. V. Ortiz, J. Cioslowski, D. J. Fox, Gaussian 09, Gaussian, Inc., Wallingford, CT, USA (2009).

[53] S. F. Boys, F. Bernardi, The calculation of small molecular interactions by the differences of separate total energies. Some procedures with reduced errors. *Mol. Phys.*, 19 (1970) 553.

[54] R. F. W. Bader, Atoms in molecules: A quantum theory, Oxford University Press, New York (1990).

[55] K. F. Biegler, J. Schonbohm, D. Bayles, AIM2000: a program to analyze and visualize atoms in molecules. *J. Comput. Chem.*, 22 (2001) 545.

[56] A. E. Reed, L. A. Curtiss, F. Weinhold, Intermolecular interactions from a natural bond orbital, donor–acceptor viewpoint. *Chem. Rev.*, 88 (1988) 899.

[57] R. G. Pearson, Chemical hardness-applications from molecules to solids, VCH-Wiley, Weinheim (1997).

[58] P. K. Chattaraj, A. Poddar, Molecular reactivity in the ground and excited electronic states through density-dependent local and global reactivity parameters. *J. Phys. Chem.*, A 103 (1999) 8691.

[59] K. D. Sen, C. K. Jorgensen, Electronegativity, Structure and Bonding, Springer Verlag, New York (1987).

[60] R. G. Parr, L. V. Szentpály, S. Liu, Electrophilicity index. *J. Am. Chem. Soc.*, 121 (1999) 1922.

[61] T. Koopmans, Über die Zuordnung von Wellenfunktionen und Eigenwerten zu den einzelnen Elektronen eines atoms. *Physica.*, 1 (1933) 104.

[62] P. Schuster, G. Zundel, The Hydrogen Bond, Recent Development in Theory and Experiment, North-Holland, Amsterdam (1976).

[63] A. Nowroozi, H. Raissi, H. Hajiabadi, P. Mohammadzadeh, Reinvestigation of intramolecular hydrogen bond in malonaldehyde derivatives: An ab

initio, AIM and NBO study. *Int. J. Quantum Chem.,* 111 (2011) 3040.
[64] E. Espinosa, E. Molins, Retrieving interaction potentials from the topology of the electron density distribution: the case of hydrogen bonds. *J. Chem. Phys.,* 113 (2000) 5686.
[65] A. Gavezzotti, L. Lo Presti, A theoretical study of chiral carboxylic acids. Structural and energetic aspects of crystalline and liquid states. *Cryst. Growth Des.,* 5(8) (2015) 3792.
[66] T. Steiner, The hydrogen bond in the solid state. *Angew. Chem. Int. Ed.,* 41 (2002) 48.
[67] C. Garau, A. Frontera, D. Quinonero, P. Ballester, A. Costa, P. M. Deya, Cation-π versus anion-π interactions: energetic, charge transfer, and aromatic aspects. *J. Phys. Chem. A*, 108 (2004) 9423.
[68] R. D. Parra, J. Ohlssen, Cooperativity in intramolecular bifurcated hydrogen bonds: an ab initio study. *J. Phys. Chem. A*, 112 (2008) 3492.
[69] M. Ziółkowski, S. J. Grabowski, J. Leszczynski, Cooperativity in hydrogen-bonded interactions: ab initio and "atoms in molecules" analyses. *J. Phys. Chem. A*, 110 (2006) 6514.
[70] L. Gonzalez, O. Mo, M. Yanez, Substituent Effects on the Strength of the Intramolecular Hydrogen Bond of Thiomalonaldehyde. *J. Org. Chem.*, 64 (1999) 2314.
[71] L. R. Domingo, M. J. Aurell, P. Pérez, R. Contreras, Quantitative characterization of the global electrophilicity power of common diene/dienophile pairs in Diels-Alder reactions. *Tetrahedron*, 5 (2002) 4417.
[72] F. J. Luque, J. M. Lopez, M. Orozco, Perspective on "Electrostatic interactions of a solute with a continuum. A direct utilization of ab initio molecular potentials for the provision of solvent effects". *Theor. Chem. Acc.*, 103 (2000) 343.
[73] T. A. Nyijime, H. F. Chahul, A. M. Ayuba, F. Iorhuna, Theoretical Study of Interaction Between Thiadiazole Derivatives on Fe(110) Surface. *J. Chem. Lett.*, 4 (2023) 86.
[74] A. P. John, A. Uzairu, G. A. Shallangwa, S. Uba, Theoretical Investigation and Design of Novel Cephalosporin Based Inhibitors of a DD-carboxypeptidase Enzyme of Salmonella typhimurium. *J. Chem. Lett.*, 4 (2023) 52-58. 10.22034/jchemlett.2022.361586.1085
[75] E. P. MAIKI, R. SUN, H. CAO, Y. HUANG, S. REN, Experimental and theoretical investigation of low salinity water injection timing in high water cut sandstone reservoirs for enhanced oil recovery. *J. Chem. Lett.*, 2 (2021) 73-81. 10.22034/jchemlett.2021.319588.1042